Oncogene
https://doi.org/10.1038/s41388-019-1021-1

ARTICLE

Identification and characterization of a BRAF fusion oncoprotein with retained autoinhibitory domains

Florian Weinberg[1,2] · Ricarda Griffin[1] · Martina Fröhlich[3] · Christoph Heining[4,5,6] · Sandra Braun[1,2] · Corinna Spohr[1,7,8] · Mary Iconomou[1] · Viola Hollek[1] · Michael Röring[1] · Peter Horak[9,10] · Simon Kreutzfeldt[9,10] · Gregor Warsow[11,12] · Barbara Hutter[3] · Sebastian Uhrig[3,13] · Olaf Neumann[10,14] · David Reuss[10,15,16] · Dieter Henrik Heiland[17,18] · Christof von Kalle[19] · Wilko Weichert[20,21] · Albrecht Stenzinger[10,14] · Benedikt Brors[3,10] · Hanno Glimm[4,5,6] · Stefan Fröhling[9,10] · Tilman Brummer[1,2,22,23]

Received: 26 November 2018 / Revised: 9 September 2019 / Accepted: 11 September 2019

Abstract

Fusion proteins involving the BRAF serine/threonine kinase occur in many cancers. The oncogenic potential of BRAF fusions has been attributed to the loss of critical N-terminal domains that mediate BRAF autoinhibition. We used whole-exome and RNA sequencing in a patient with glioblastoma multiforme to identify a rearrangement between *TTYH3*, encoding a membrane-resident, calcium-activated chloride channel, and *BRAF* intron 1, resulting in a TTYH3–BRAF fusion protein that retained all features essential for BRAF autoinhibition. Accordingly, the BRAF moiety of the fusion protein alone, which represents full-length BRAF without the amino acids encoded by exon 1 ($BRAF^{\Delta E1}$), did not induce MEK/ERK phosphorylation or transformation. Likewise, neither the TTYH3 moiety of the fusion protein nor full-length TTYH3 provoked ERK pathway activity or transformation. In contrast, TTYH3–BRAF displayed increased MEK phosphorylation potential and transforming activity, which were caused by TTYH3-mediated tethering of near-full-length BRAF to the (endo)membrane system. Consistent with this mechanism, a synthetic approach, in which $BRAF^{\Delta E1}$ was tethered to the membrane by fusing it to the cytoplasmic tail of CD8 also induced transformation. Furthermore, we demonstrate that TTYH3–BRAF signals largely independent of a functional RAS binding domain, but requires an intact BRAF dimer interface and activation loop phosphorylation sites. Cells expressing TTYH3–BRAF exhibited increased MEK/ERK signaling, which was blocked by clinically achievable concentrations of sorafenib, trametinib, and the paradox breaker PLX8394. These data provide the first example of a fully autoinhibited BRAF protein whose oncogenic potential is dictated by a distinct fusion partner and not by a structural change in BRAF itself.

Introduction

The serine/threonine kinase BRAF has become a major drug target in various malignancies [1]. Oncogenic mutations of the *BRAF* gene can be subdivided into gene fusions generated by intra- or interchromosomal rearrangements [2] and single-nucleotide variations or small insertions/deletions that result in full-length BRAF proteins with altered kinase activity [3, 4]. How these alterations subvert the intrinsic regulation of BRAF and generate potent oncoproteins is best understood from a structural perspective.

Like all RAF family members, BRAF possesses three conserved regions (CR) that encompass structurally defined subdomains [5, 6]. The CR1 is located C-terminal to the N-terminal BRAF-specific region (NBSR) and contains two subdomains, the RAS-binding domain (RBD) and the

These authors share first authorship: Florian Weinberg, Ricarda Griffin

These authors contributed equally: Hanno Glimm, Stefan Fröhling, Tilman Brummer

Supplementary information The online version of this article (https://doi.org/10.1038/s41388-019-1021-1) contains supplementary material, which is available to authorized users.

✉ Stefan Fröhling
stefan.froehling@nct-heidelberg.de

✉ Tilman Brummer
tilman.brummer@mol-med.uni-freiburg.de

Extended author information available on the last page of the article

Published online: 26 September 2019

cysteine-rich domain (CRD), which are both involved in RAS binding. The CR2 harbors several phosphorylation sites of which S365 plays an important role for maintaining BRAF in an autoinhibited state by serving as 14–3–3 binding site. The relevance of the CR2 for autoinhibition is demonstrated by the observation that mutations affecting 14–3–3 binding have been found in ARAF, BRAF, and CRAF in cancer and RASopathies [7], and that the exons encoding the N-terminal moiety of RAF kinases (NBSR, CR1, and CR2) are deleted in viral *raf* oncogenes and in the growing spectrum of oncogenic *RAF* fusion genes [5]. The CR2 is followed by the hinge region (HR), which contains phosphorylation site clusters negatively controlling BRAF signaling and stability [7]. The CR3 encompasses the N-region, an area critical for kinase activity, and the kinase domain itself. The kinase domain contains several residues involved in RAF dimerization, including R509 at the dimer interface (DIF). The DIF plays a key role in dimerization-mediated allosteric transactivation of a receiver kinase molecule by an activated RAF protein [5, 8–10]. In addition to the DIF, 14–3–3 proteins binding to the C-terminal end of CR3 also contribute to dimer formation [6]. Following membrane recruitment by RAS, BRAF is fully activated by conformational changes induced by dimerization and phosphorylation of the $T^{599}VKS^{602}$ motif within the activation loop (AL) (see [11] and references therein). RAF dimerization is also critical for the formation of large active signaling complexes [8, 12] and MEK phosphorylation [13].

AL phosphorylation is mimicked by the most common BRAF mutation, V600E, which generates a mutation-specific salt bridge stabilizing the active conformation of the kinase domain and thereby produces an oncoprotein exempted from multiple layers of positive and negative regulation [8]. In contrast, more than 50 BRAF fusion oncoproteins described to date [2] are generated by intra- or interchromosomal rearrangements taking place within the introns preceding exons 9, 10, or 11. Although the N-terminal fusion partners are derived from proteins of various functions and subcellular localization, all BRAF fusion proteins share an intact CR3 and the loss of the autoinhibitory N-terminal moiety consisting of the NBSR, RBD, CRD, CR2 and, in some cases, the HR. As the autoinhibitory moiety needs to be displaced by active RAS to induce dimerization of the kinase domains in BRAF wild-type proteins, BRAF fusion proteins display increased homodimerization potential [14] and are thus in a state of preactivation, in which they require only transactivation for full activity [11]. Compared with point mutants such as $BRAF^{V600E}$, BRAF fusion proteins express unmutated kinase domains and presumably exhibit a variety of conformational states. This might explain why BRAF fusions display a reduced affinity toward small-molecule inhibitors such as vemurafenib that were designed to target the active conformation of $BRAF^{V600E}$ [15]. Moreover, the high dimerization potential of BRAF fusion proteins counteracts the uptake of vemurafenib or its tool compound PLX4072 [14, 16]. Chromosomal rearrangements leading to structurally similar oncoproteins have been described for the human *RAF1* locus [17–19], although recent data suggest distinct properties and RAF inhibitor sensitivities of BRAF and RAF1 fusion proteins [20].

Apart from melanoma and hairy cell leukemia [1], BRAF alterations are particularly frequent in specific types of low-grade glioma [14, 19, 21, 22], which probably reflects the critical role of the kinase in macroglia [11, 23, 24]. $BRAF^{V600E}$ also occurs at lower frequencies (2–12%) in highly malignant glioblastoma (GBM), in particular in the epithelioid subtype (54%). BRAF fusions, however, have been rarely reported in GBM (0.5%) [25, 26]. Here we report a unique case of GBM, in which an intrachromosomal rearrangement between *TTYH3* and *BRAF* produced two unusual BRAF fusion proteins. Of particular interest, we identified and characterized a novel BRAF fusion that exhibits transforming activity despite the presence of the autoinhibitory N-terminal moiety.

Results

Identification of complex BRAF alterations in a GBM patient

This study originated from the genetic analysis of a 65-year-old woman who had been diagnosed with left frontal GBM. Treatment consisted of surgical resection and intraoperative radiation, followed by external-beam radiation and concurrent and adjuvant temozolomide. To identify therapeutically tractable molecular lesions, the patient was enrolled in the MASTER (Molecularly Aided Stratification for Tumor Eradication Research) program, a multi-institutional, genomics-guided precision oncology platform for adults with advanced-stage cancer across all histologies [27]. Whole-exome sequencing (WES) of tumor tissue and a matched blood sample revealed no typical GBM-associated alterations [28, 29], except for two *PIK3R1* mutations (Supplementary Table S1). Both mutations, G376R, which has been recurrently found in GBM, and H407Q are largely uncharacterized. Further analysis of the WES data and subsequent validation by Sanger sequencing revealed an acquired complex rearrangement of chromosome 7 that resulted in two distinct gene fusions involving *TTYH3* on chromosome 7p22 and *BRAF* on chromosome 7q34. The first fusion was caused by a pericentric inversion between intron 13 of *TTYH3* and intron 1 of *BRAF* (Fig. 1a and Supplementary Fig. S1a). The second fusion

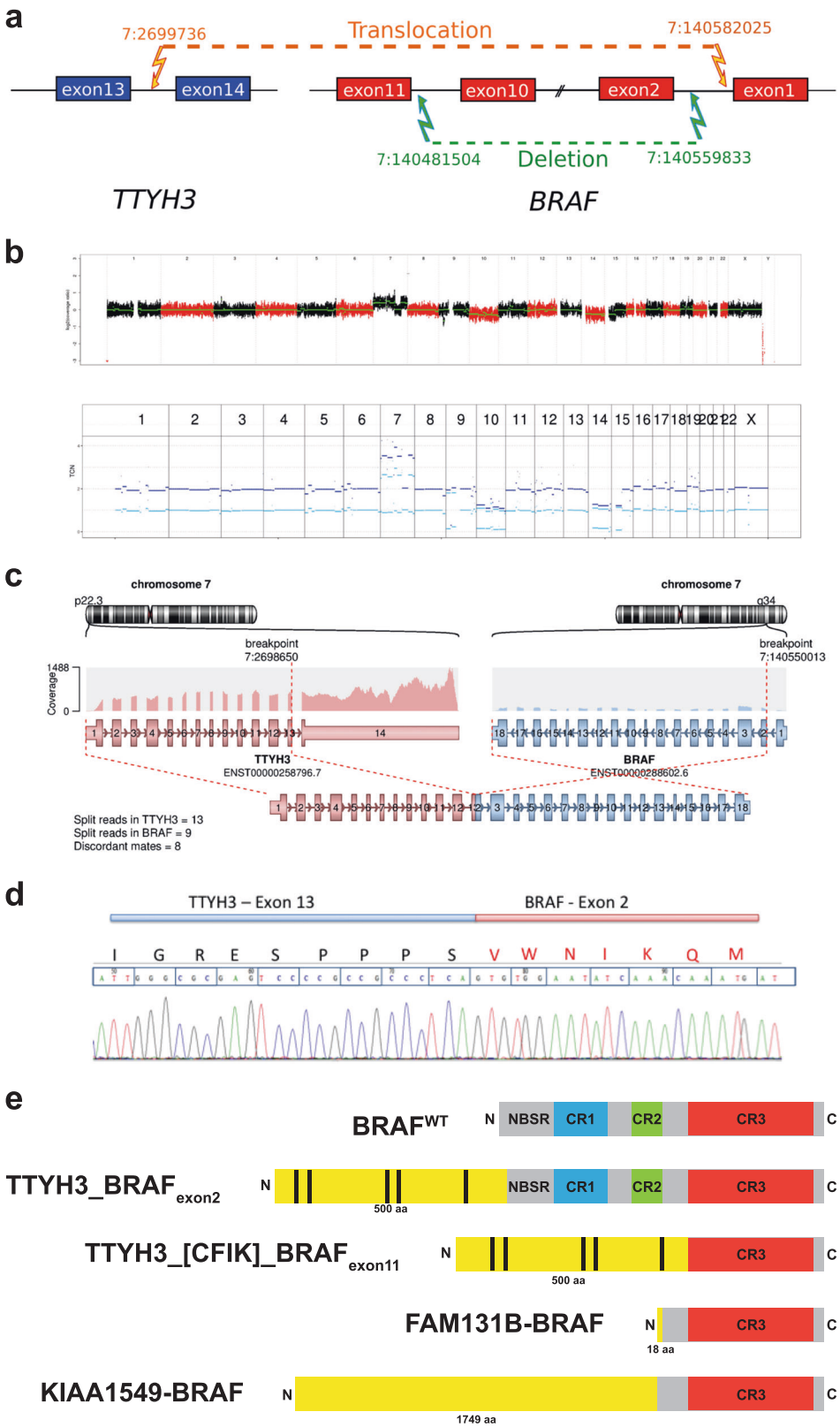

Fig. 1 Complex genomic rearrangement of chromosome 7 in a patient with GBM. **a** Schematic of the genomic rearrangements leading to TTYH3–BRAF fusion transcripts with the translocation event (orange) preceding the deletion (green). **b** DNA copy number estimation analysis showing amplification of multiple regions on chromosome 7, which include the *TTYH3* and *BRAF* loci. **c** Schematic of the *TTYH3_BRAF*$_{exon2}$ fusion gene and the resulting chimeric transcript. **d** Validation of the chimeric *TTYH3_BRAF*$_{exon2}$ transcript by Sanger sequencing. **e** Cartoon illustrating the primary structures of wild-type BRAF (BRAF^{WT}; with its structural features outlined in the introduction) and the two TTYH3-BRAF fusion proteins. For comparison, the primary structures of the FAM131B–BRAF [19] and KIAA1549–BRAF [21] oncoproteins, which significantly differ in the length of their non-BRAF component, is shown. The non-BRAF moiety of all four fusion proteins is depicted in yellow. The presumptive transmembrane passes of TTYH3 are indicated by black vertical bars. Note that only TTYH3_BRAF$_{exon2}$ retains the structural features involved in BRAF auto-inhibition

additionally harbored a genomic deletion ranging from intron 1 to intron 10 of *BRAF* (Fig. 1a and Supplementary Fig. S1b). Copy number estimation analyses performed with CNVkit showed that the *TTYH3* and *BRAF* loci were present with 3.4 and 3.6 copies, respectively (Fig. 1b and Supplementary Table S1).

RNA sequencing showed that both fusions were expressed based on the detection of two distinct transcripts supported by similar numbers of split reads (Fig. 1c and Supplementary Fig. S1c). The *TTYH3_BRAF*$_{exon2}$ transcript, which is explained by the inversion, results in a multipass transmembrane protein, in which a 500-amino acid peptide encoded by exons *TTYH3* 1–13 is fused at its cytoplasmic C-terminus to an almost full-length BRAF protein. Unlike typical BRAF fusion oncoproteins consisting mainly of the CR3, the BRAF component of TTYH3_BRAF$_{exon2}$ only lacks the 46 amino acids encoded by exon 1 (Fig. 1c–e). TTYH3 is the human ortholog of the *Drosophila* flightless protein and appears to be most abundant in the brain (https://gtexportal.org/home/gene/TTYH3) [30]. It belongs to the small family of Tweety/TTYH putative large-conductance Ca^{2+}-activated chloride channels and has been recently, together with TTYH1/2, identified as the major volume-regulated anion channel (VRAC) in astrocytes [31]. The topology of all three TTYH proteins has not been fully elucidated, and four to six transmembrane (TM) passes have been proposed for these channel proteins [30–33]. Very recent functional and topology prediction tools suggest four TM passes for TTYH1 and five for TTYH2 and TTYH3 [31]. The fusion with near-full-length BRAF occurs 88 amino acids C-terminal of the last TM pass in the cytoplasmic part of TTYH3 and deletes the last 23 amino acids of TTYH3. Compared with the growing spectrum of oncogenic BRAF fusions, in which typically the kinase domain and some flanking residues are present [2], the TTYH3_BRAF$_{exon2}$ fusion is highly unusual, as it retains all aforementioned features required for auto-inhibition, such as the NBSR, RBD, the CRD, CR2, and HR. Thus, it was conceivable that the TTYH3_BRAF$_{exon2}$ fusion protein remained stringently controlled and rather represented a passenger alteration than an oncogenic driver.

The second fusion connects *TTYH3* exon 13 to an intronic region upstream of *BRAF* exon 11, resulting in a *TTYH3_[CFIK]_BRAF*$_{exon11}$ fusion transcript (Fig. 1e and Supplementary Figs. S1c and S2). This transcript generates a chimeric protein, in which TTYH3 is fused to the CR3 domain of BRAF via a short peptide linker inserting the amino acid sequence CFIK. The CFIK sequence is partly derived from the intron sequence of *BRAF*. In sharp contrast to TTYH3_BRAF$_{exon2}$, the TTYH3_[CFIK]_BRAF$_{exon11}$ fusion protein has lost the entire autoinhibitory moiety, and the BRAF component starts with a sequence encoded by the first exon corresponding to the CR3 (Fig. 1e and Supplementary Fig. S2; [34]). Thus, the primary structure of the BRAF component of this fusion protein is highly similar to that of the many other oncogenic fusions containing sequences derived from *BRAF* exons 11 to 18, e.g., KIAA1549–BRAF (Fig. 1e), and is almost certainly oncogenic [2, 18, 19, 21, 35, 36].

The existence of the *TTYH3_[CFIK]_BRAF*$_{exon11}$ transcript implies that the inversion occurred first, followed by the deletion of the genomic region spanning *BRAF* exons 2–10. We cannot rule out that the second rearrangement represents a purely subclonal event. However, the presence of more than two copies of *TTYH3* and *BRAF* in the DNA and the fact that both fusion transcripts are supported by a similar number of split reads in the RNA (see Fig. 1c and Supplementary Fig. S1c) also allow for the possibility that both fusions coexist within the same cells.

Functional characterization of TTYH3_BRAF$_{exon2}$

As the TTYH3_BRAF$_{exon2}$ fusion protein (from here on designated as TTYH3–BRAF^{WT}) retains all known autoinhibitory features of BRAF, we asked whether it constitutes an oncogenic driver in its own right, in addition to the oncogenic TTYH3_[CFIK]_BRAF$_{exon11}$ fusion. We generated a series of bicistronic pMIBerry expression vectors encoding C-terminally Myc/His-tagged TTYH3-BRAF^{WT} (or mutants thereof described below) and the red fluorescent protein dsRed2 [8]. The Myc/His tag was placed at the C-terminus of BRAF to avoid interference with membrane insertion of the TTYH3 moiety and because this tag and its position do not compromise BRAF function [8, 11]. To distinguish effects caused by *BRAF* exon 1 deletion from those arising from the fusion of BRAF to the C-terminus of TTYH3, we generated an expression vector for a BRAF protein lacking the exon 1-encoded sequence and the entire TTYH3 moiety (BRAF$^{\Delta E1}$). As additional controls, we constructed expression vectors for C-terminally Myc-tagged full-length TTYH3 (TTYH3^{FL}) and its TTYH3$^{\Delta E14}$ variant, which lacks the amino acids encoded by *TTYH3* exon 14 and hence represents the Tweety component of TTYH3-BRAF^{WT}.

As *TTYH3* encodes a membraneous protein, we first investigated the subcellular localization of TTYH3^{FL}, TTYH3$^{\Delta E14}$ and TTYH3-BRAF^{WT} in the GBM cell line LN-229ecoR, which is derived from LN-229 [37] and stably expresses the receptor for ecotropic retrovirus infection (ecoR). As shown in Fig. 2a, BRAF^{WT} displayed the expected predominantly cytoplasmic localization, while TTYH3^{FL} and TTYH3$^{\Delta E14}$ were concentrated in puncta found at the plasmamembrane and intracellularly, in particular in the perinuclear region that is rich in endomembrane system components and hence contains most of the cellular membranes. This staining pattern of TTYH3, which had not been investigated previously, is reminiscent of that reported for the structurally related TTYH1 and TTYH2 proteins using antibodies against the endogenous protein or green fluorescent protein tags [32, 33, 38, 39]. Importantly, TTYH3–BRAF^{WT} also displayed a membraneous and punctate staining pattern in LN-229ecoR GBM cells. Puncta

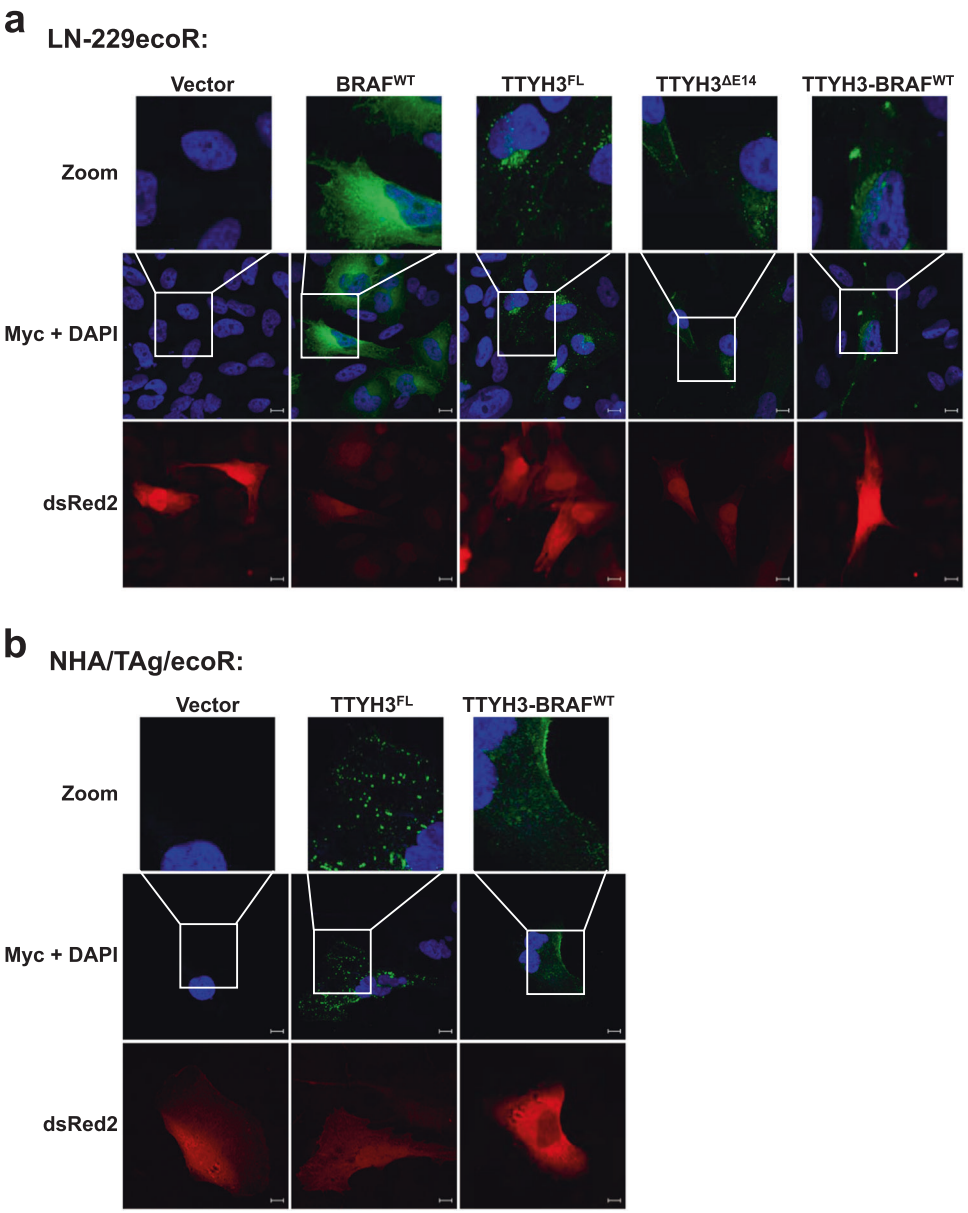

Fig. 2 TTYH3–BRAF^{WT} is localized to membraneous structures. **a** Confocal immunofluorescence microscopy of LN-229ecoR cells and NHA/TAg/ecoR cells (**b**) infected with the indicated pMIBerry constructs and stained with anti-Myc antibody (green) to reveal the localization of TTYH3, BRAF, and TTYH3–BRAF^{WT} proteins. Nuclei were counterstained with DAPI. Red fluorescence indicates the expression level of dsRed2 encoded by the pMIBerry retroviral vector. Scale bar = 10 µm

were also observed using an antibody recognizing endogenous TTYH3 (Supplementary Fig. 3a). Similar staining patterns were obtained in experiments using Simian Virus 40 large T antigen (TAg)-immortalized normal human astrocytes (NHA/TAg/ecoR; [40]), another GBM cell line, GSC-233, and COS-7 cells, in which we also included BRAF^{V600E}, BRAF$^{\Delta E1}$ and point mutants of TTYH3–BRAF^{WT} described in detail below (Fig. 2b, Supplementary Figs. S3b and S4a–c). COS-7 cells were chosen due to their high cytoplasm/nucleus ratio, facilitating subcellular localization studies. Again, BRAF^{WT}, BRAF^{V600E}, and BRAF$^{\Delta E1}$ displayed cytoplasmic localization, while all TTYH3 and TTYH3–BRAF proteins localized to membranous or vesicular structures. In summary, the stainings in the four cell lines show that the typical cytoplasmic staining of BRAF is dramatically altered by the TTYH3 fusion partner, indicating that the N-terminal chloride channel extension tethers BRAF to the (endo) membrane system.

To confirm correct expression of the various BRAF proteins and to assess their signaling potential, we next introduced them into TAg-immortalized murine embryonic fibroblasts (MEFs), which were later also used to assess transforming activity, NHA/TAg/ecoR as a nontransformed cell type of glial origin, and into the HEK293 derivative Plat-E [8, 41] that facilitates protein biochemistry assays. In these assays, all BRAF proteins displayed the expected molecular mass and BRAF^{V600E}, used as positive control,

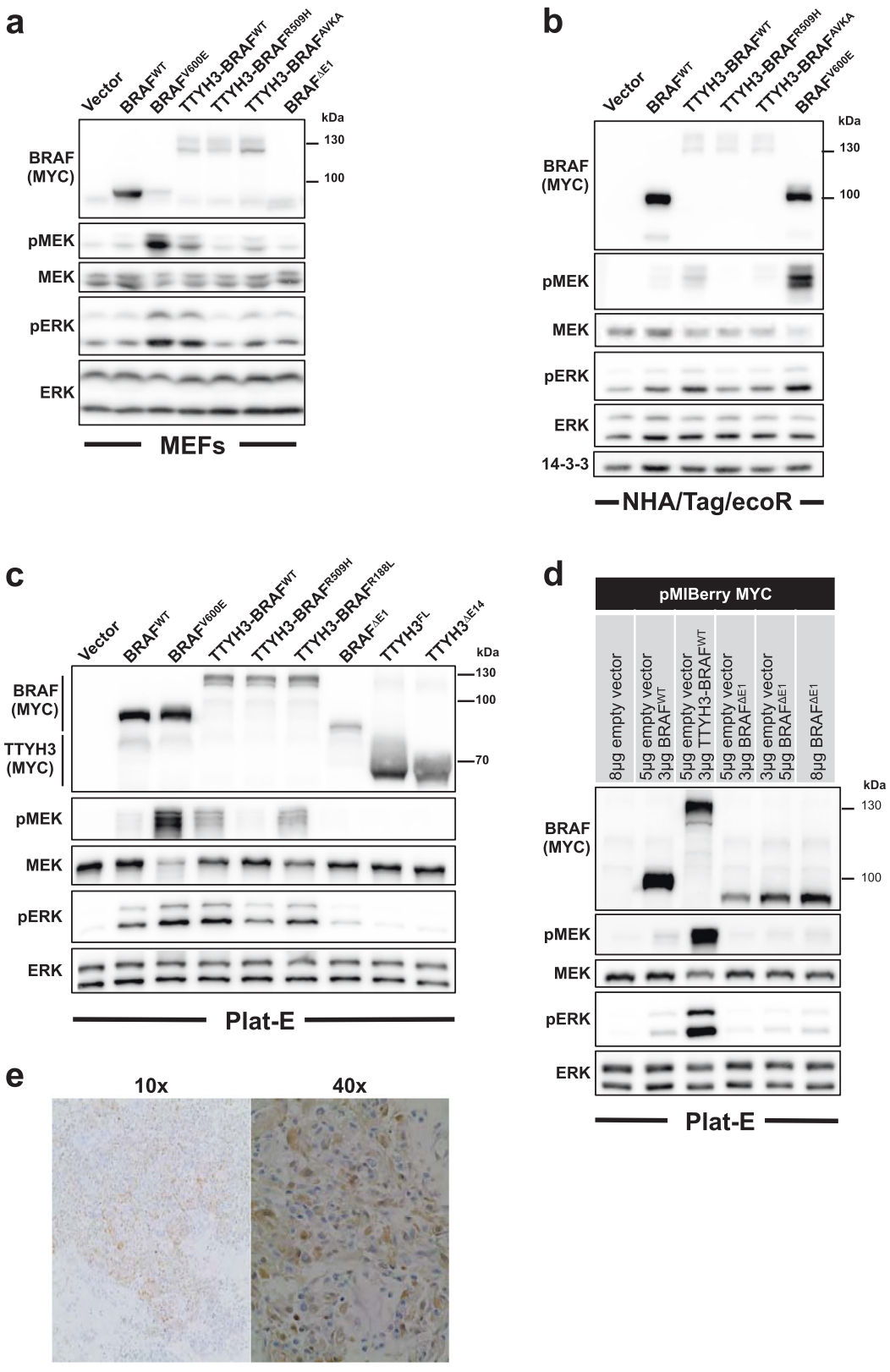

induced prominent MEK/ERK phosphorylation (Fig. 3a–d). Interestingly, the amount of Myc-tagged TTYH3–BRAF^{WT} appears lower than that of wild-type BRAF (BRAF^{WT}) in all three cell types. This could reflect a lower expression of the fusion protein compared with BRAF^{WT} or could be caused by a more inefficient transfer of TTYH3–BRAF^{WT}

◀ **Fig. 3** TTYH3 increases BRAF activity. **a** MEFs were infected with the indicated constructs and total cell lysates (TCLs) were analyzed by western blotting with the indicated antibodies two days later. TTYH3–BRAF^{WT} strongly induces MEK and ERK phosphorylation in a DIF- and AL-dependent manner. **b** TCLs of NHA/TAg/ecoR cells infected with the indicated constructs were subject to western blotting using the indicated antibodies. **c**, **d** Plat-E cells were transfected with the indicated constructs and TCLs were analyzed by western blotting with the indicated antibodies. **d** Increasing amounts of BRAF$^{\Delta E1}$ only marginally induce phosphorylation of MEK or ERK compared to empty vector control cells. **e** Immunohistochemistry reveals pERK positive GBM tissue

(compared with BRAF^{WT}) during western blotting due to its increased size and presumed glycosylation, a modification that has been described for TTYH3 and is known to affect its electrophoretic migration. Indeed, the doublet of TTYH3–BRAF^{WT} is reminiscent of the SDS-PAGE migration pattern of differentially glycosylated forms of TTYH3 [30, 33]. Importantly, all three cell types expressing TTYH3–BRAF^{WT} exhibited MEK/ERK phosphorylation levels considerably higher than those expressing BRAF^{WT} but lower than those expressing the high-activity BRAF^{V600E} mutant (Fig. 3a–d). Commensurate with these findings, tumor tissue from the GBM patient stained positive for phospho-ERK (Fig. 3e).

The signaling potential of TTYH3–BRAF^{WT} was reduced by the AVKA mutation, which prevents phosphorylation of T599 and S602 in the BRAF AL [11], and even more strongly by the R509H mutation, which impairs DIF function and homodimerization of BRAF [8] (Fig. 3a–c). In contrast, leucine substitution of the evolutionarily conserved RBD residue R188, which prevents RAS-induced RAF activation (see [8] and references therein), had no discernible effect on the MEK/ERK phosphorylation potential of TTYH3–BRAF^{WT} (Fig. 3c).

Next, we asked whether the loss of *BRAF* exon 1 by the fusion might cause the elevated MEK/ERK phosphorylation potential of TTYH3–BRAF^{WT}. As shown in Fig. 3a–c, BRAF$^{\Delta E1}$ provoked a level of MEK/ERK phosphorylation below that of BRAF^{WT}-expressing cells. However, in various experiments involving different cell types, we noticed that it was difficult to achieve the same degree of BRAF$^{\Delta E1}$ overexpression as for BRAF^{WT} or TTYH3–BRAF^{WT}, complicating a direct comparison of these two variants. Therefore, we transfected increasing amounts of the BRAF$^{\Delta E1}$ expression vector and compared the effects of various expression levels with those of TTYH3–BRAF^{WT}. Yet, even higher levels of BRAF$^{\Delta E1}$ did not induce the prominent MEK/ERK phosphorylation triggered by TTYH3–BRAF^{WT} (Fig. 3d). Thus, the increased signaling potential of TTYH3–BRAF^{WT} cannot be attributed to the loss of *BRAF* exon 1.

Recently, Jung et al. reported that TTYH1 drives brain colonization of gliomas [38], suggesting that the TTYH3 component might activate MEK/ERK. However, we observed no induction of MEK/ERK phosphorylation upon overexpression of TTYH3^{FL} or TTYH3$^{\Delta E14}$, which corresponds to the TTYH3 moiety in TTYH3–BRAF^{WT} (Fig. 3c).

Typical BRAF fusion proteins and BRAF oncoproteins consisting almost exclusively of the kinase domain, e.g., the vemurafenib-induced and resistance-conferring splice variant BRAF$^{\Delta E2\text{-}E10}$, display enhanced DIF-dependent homodimerization [14, 16]. As TTYH3–BRAF^{WT} retains autoinhibitory domains that are usually displaced by RAS prior to dimerization [6] and whose absence in N-terminally truncated BRAF oncoproteins contributes to their dimerization behavior [13, 42], we asked whether this unsual BRAF fusion protein engages in dimerization. Therefore, we coexpressed Myc- and HA-tagged BRAF constructs in Plat-E cells and assessed the amount of HA-tagged BRAF proteins in anti-Myc immunoprecipitates, as described previously [8]. As shown in Supplementary Fig. 5a, TTYH3–BRAF^{WT} co-immunoprecipitated with BRAF^{WT} and BRAF$^{\Delta E2\text{-}E10}$ (lane 4 and 9), which was included as a positive control for increased dimerization [42]. In contrast, TTYH3–BRAF^{R509H} failed to copurify detectable amounts of BRAF^{WT} and BRAF$^{\Delta E2\text{-}E10}$ (lane 5 and 10), indicating that an intact DIF is critical for homodimerization of TTYH3–BRAF^{WT}, as it was demonstrated for BRAF [8, 9, 13]. Next, we addressed the homo- and heterodimerization potential of TTYH3–BRAF^{WT} with endogenously expressed RAF proteins in NHA/TAg/ecoR cells, as this experimental system is more closely related to GBM. To enrich for RAF dimers, we pretreated NHA/TAg/ecoR with sorafenib, which promotes dimer-dependent BRAF complexes [8, 12, 43] and contributes to their stability by quenching ERK-mediated feedback loops contributing to dimer disruption [44, 45]. As shown in Supplementary Fig. S5b, sorafenib induced heterodimers between BRAF^{WT} or TTYH3–BRAF^{WT} and RAF1 or ARAF. Given their prominent size difference, we could also detect a sorafenib-induced increase in homodimers between TTYH3–BRAF^{WT} and endogenous BRAF (Supplementary Fig. S5c). Moreover, the R509H mutation impaired the formation of sorafenib-induced heterodimers between TTYH3–BRAF and endogenous ARAF and BRAF, while heterodimerization between the fusion protein and RAF1 was not affected (Supplementary Fig. S5b, c). This result is reminiscent of our previous data showing that the R509H substitution alone is not sufficient to impair heterodimer formation and/or stability between BRAF and RAF1 in MEFs and RAS-driven colorectal cancer cells [8]. Thus, our data show that TTYH3–BRAF engages in homo- and heterodimerization and that an intact DIF is required for its ability to induce MEK phosphorylation.

TTYH3–BRAF^{WT} transforms MEFs in a DIF- and AL-dependent manner

Next, we assessed the transformation potential of the various BRAF proteins by infecting MEFs with different pMIBerry bicistronic vectors encoding dsRed2 in addition to BRAF [8]. As shown in Fig. 4a–c, MEFs infected with the empty vector or BRAF^{WT} remained contact-inhibited and fully integrated in the monolayer, while cells expressing TTYH3–BRAF^{WT} formed foci. In contrast, TTYH3–BRAF^{AVKA} and TTYH3–BRAF^{R509H} failed to induce a significant number of foci (Fig. 4b), while TTYH3–BRAF^{R188L} was still able to induce MEF transformation, albeit with reduced efficiency (Fig. 4c). In agreement with Fig. 3c, BRAF$^{\Delta E1}$, TTYH3^{FL}, TTYH3$^{\Delta E14}$, and BRAF^{R188L} induced no foci (Fig. 4a–d). Thus, the elevated signaling and transformation potential of TTYH3–BRAF^{WT} is caused by the tethering of an

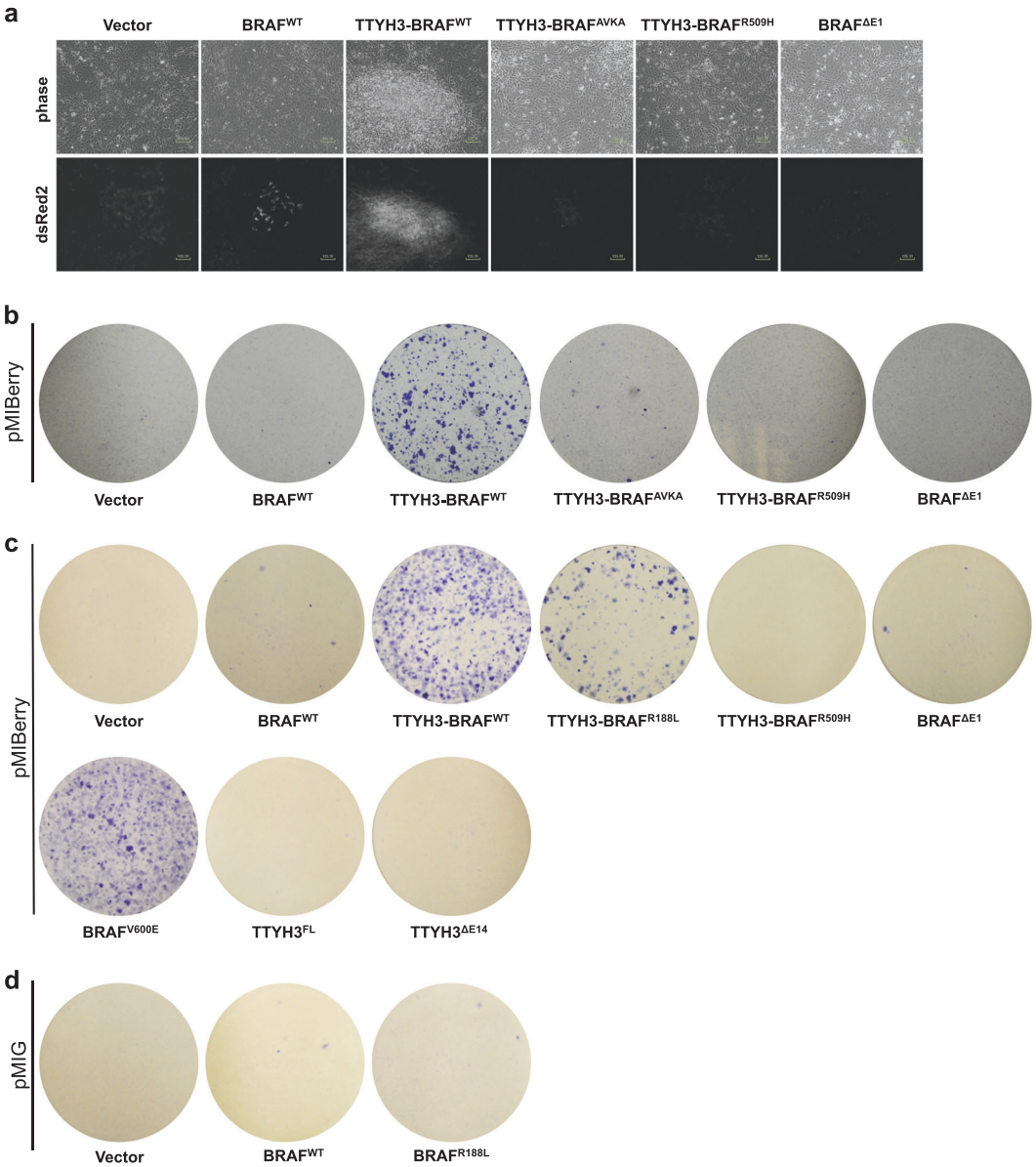

Fig. 4 TTYH3–BRAF^{WT} transforms MEFs due to membrane tethering and in a DIF- and AL-dependent manner. **a–d** Focus assay of MEFs infected with the indicated retroviral constructs. TTYH3–BRAF^{WT} induces the formation of foci, which is abrogated by mutation of the DIF (R509H) or the AL (AVKA) and partially inhibited by blocking the RAS/RAF interaction (R188L). **a** Phase contrast and fluorescence images of infected MEFs growing as monolayer or forming single foci. Scale bars, 100 µm. **b** Plates were fixed and stained with Giemsa solution. Focus formation reflects the loss of contact inhibition upon expression of oncogenic BRAF. Data represent one of at least three independent transduction experiments. Experiments in **b** and **c** represent independent experiments, in which plates infected with pMIBerry, pMIBerry/BRAF, and pMIBerry/TTYH3-BRAF served as reference plates for the individual experiments. **d** MEFs were infected with the indicated pMIG constructs [8] to demonstrate that BRAF^{R188L} does not transform MEFs

almost full-length and otherwise nontransforming BRAF protein to TTYH3 and not by the TTYH3 moiety itself. Furthermore, these activities of TTYH3–BRAF^{WT} were less reliant on RAS binding but strongly dependent on an intact DIF and AL.

Our concept that BRAF$^{\Delta E1}$ only becomes transforming upon membrane tethering could be supported by the removal of the membrane-targeting sequences in the TTYH3 moiety and relocalization of the fusion protein to the cytoplasm. However, as TTYH proteins contain at least five TM passes [30, 32, 33] and as each pass is introduced by an internal and undefined signal peptide, it would be extremely difficult to prevent membrane targeting of TTYH3–BRAF^{WT} by a mutagenesis approach without causing drastic alterations to the primary structure of the channel. Therefore, we applied a synthetic approach and fused BRAF$^{\Delta E1}$ to the last amino acid at the C-terminus of human CD8α (Fig. 5a; termed CD8 in the following), a typical type I TM protein with a well-defined signal peptide [46]. As shown in Fig. 5b, c, the N-terminal CD8 extension of BRAF$^{\Delta E1}$ conferred strong transformation potential and induced prominent MEK/ERK phosphorylation. Expression of CD8 did not cause foci. We further dissected the transforming mechanism of CD8–BRAF$^{\Delta E1}$ by replacing the intermolecular disulfide bond forming cysteines 164 and 181 by serine residues [47] and by deleting the N-terminal signal peptide of CD8 [46]. The former mutant should rule out that the transforming activity of CD8–BRAF$^{\Delta E1}$ is caused by dimerization mediated via the extracellular CD8 moiety, while the latter, termed as CD8$^{\Delta SP}$–BRAF$^{\Delta E1}$ in the following, was designed to prevent membrane insertion of CD8–BRAF$^{\Delta E1}$. Importantly, CD8^{C181S}–BRAF$^{\Delta E1}$ and CD8$^{C164S/C181S}$–BRAF$^{\Delta E1}$ were still transforming and caused MEK phosphorylation, suggesting that CD8 homodimerization is not responsible for the transforming activity of this fusion protein (Fig. 5b, c). Unfortunately, CD8$^{\Delta SP}$–BRAF$^{\Delta E1}$ was only very weakly expressed, preventing a conclusion regarding its transforming ability (Fig. 5c). This suggests that the CD8–BRAF$^{\Delta E1}$ protein is unstable, e.g., due to unproper folding of the CD8 immunoglobulin variable-like extracellular domain in the cytoplasm. Next, we analyzed the subcellular localization of the CD8–BRAF$^{\Delta E1}$ fusion protein in LN-229ecoR GBM cells. As shown in Supplementary Fig. S6a, CD8–BRAF$^{\Delta E1}$ localized to endomembrane structures, and its staining pattern was distinct from the diffuse appearance of BRAF^{WT}. Commensurate with its low expression in MEFs (Fig. 5c), CD8$^{\Delta SP}$–BRAF$^{\Delta E1}$ could not be detected by anti-Myc staining in GBM cells, despite prominent expression of dsRed2, which is derived from the same bicistronic transcript. This further supports our assumption that CD8$^{\Delta SP}$–BRAF$^{\Delta E1}$ is unstable.

Using extra- and intracellular stainings for human CD8α, we also measured the degree of plasma membrane exposure of CD8–BRAF$^{\Delta E1}$ (Supplementary Fig. S6b). Interestingly, while the majority of cells transduced with the expression construct for CD8α displayed this molecule on their surface, CD8–BRAF$^{\Delta E1}$ was only exposed on the plasma membrane in a few percent of dsRed2-expressing cells. This suggests that the BRAF$^{\Delta E1}$ moiety might interfere with C-terminal trafficking signals promoting anterograde transport of CD8 [48]. In summary, our synthetic approach using human CD8α provides further evidence that (endo)membrane residency of the BRAF$^{\Delta E1}$ moiety is necessary and sufficient for transformation.

Effects of TTYH3–BRAF^{WT} in GBM cells

So far, we had analyzed the biological activity of TTYH3–BRAF^{WT} and mutants thereof mainly in immortalized non-GBM cell models. These heterologous systems are well-suited for the characterization of oncoproteins, in particular for transformation assays that require non-transformed cells as a basis. Their potential drawback, however, is that they do not always reflect the histological context, in which the oncoproteins were identified. Therefore, we analyzed the effects of TTYH3–BRAF^{WT} in ecoR-expressing pools of the GBM cell lines LN-229 and GSC-233. As the former is a well-defined GBM line with moderate ERK phosphorylation levels that can be further induced by EGF [37, 49, 50], we originally considered this cell line as suitable to discern signaling differentials between the various BRAF proteins. The latter represents a GBM stem-like cell [51] and was chosen as a cell line model that is even closer to primary GBM.

First, we analyzed the effects of the various BRAF proteins and their controls in LN-229ecoR cells. Interestingly, the MEF-transforming BRAF^{V600E}, TTYH3–BRAF^{WT}, and CD8–BRAF$^{\Delta E1}$ proteins induced a neurite-like morphology with slender processes and proliferation arrest as reflected by the decline of dsRed2-expressing cells over time (Fig. 6a, b). In contrast, LN-229ecoR cells infected with the empty control vector or expressing CD8 or BRAF^{WT} continued to proliferate and maintained a normal morphology. This suggested that excessive BRAF activity triggers a differentiation process, a hypothesis that needs to be further addressed in future studies, but that is reminiscent of the well-described neuritogenic effects of oncogenic RAS/ERK pathway components in PC12 cells [52] and KLF6-induced neuronal differentiation observed in LN-229 cells [53]. It should be mentioned that RAS/ERK pathway activity in LN-229 cells is presumably already elevated due to a *PTPN11* mutation encoding the SHP2^{A72S} gain-of-function mutant that has been found in Noonan syndrome [54], glioma, and myeloid neoplasia (https://cancer.sanger.ac.uk/cosmic/mutation/overview?id=1948744). Indeed, the differential in MEK/ERK phosphorylation in LN-229ecoR cells expressing BRAF^{WT}, TTYH3–BRAF^{WT}, or CD8–BRAF$^{\Delta E1}$

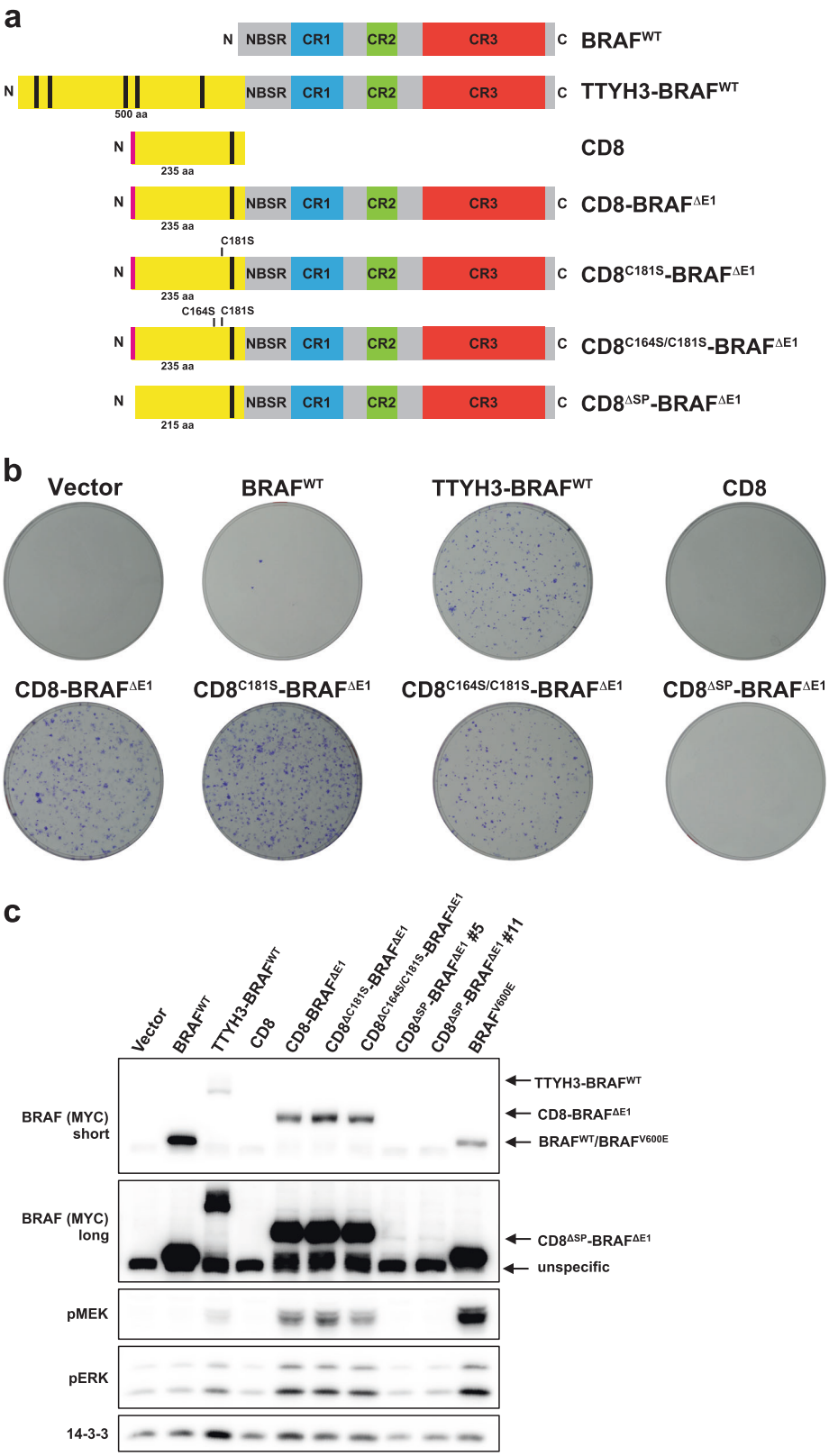

Fig. 5 Membrane tethering of the BRAF component present in TTYH3–BRAF^{WT} by human CD8 is sufficient to confer transforming properties. **a** Cartoon showing the various CD8 fusion proteins. The presumptive transmembrane passes of TTYH3 and CD8 are indicated by black vertical bars. The pink vertical bar specifies the signal peptide of CD8 and the cysteine-to-serine substitutions preventing CD8 dimerization are also indicated. **b** Focus assay as described for Fig. 4b using the indicated constructs. Data represent one of at least three independent transduction experiments. **c** Western blot analysis of MEFs infected with the indicated retroviral vectors. CD8$^{\Delta SP}$–BRAF$^{\Delta E1}$ #5 and #11 represent two independently generated plasmid clones

was less pronounced than in MEFs (Fig. 5c) and GSC-233ecoR cells, in which the ERK pathway was strongly induced by the active BRAF proteins (Supplementary Fig. S7). Together with the observed morphological effects and depletion of LN-229ecoR cells expressing transforming BRAF mutants (Fig. 6), this makes them unsuitable for extensive

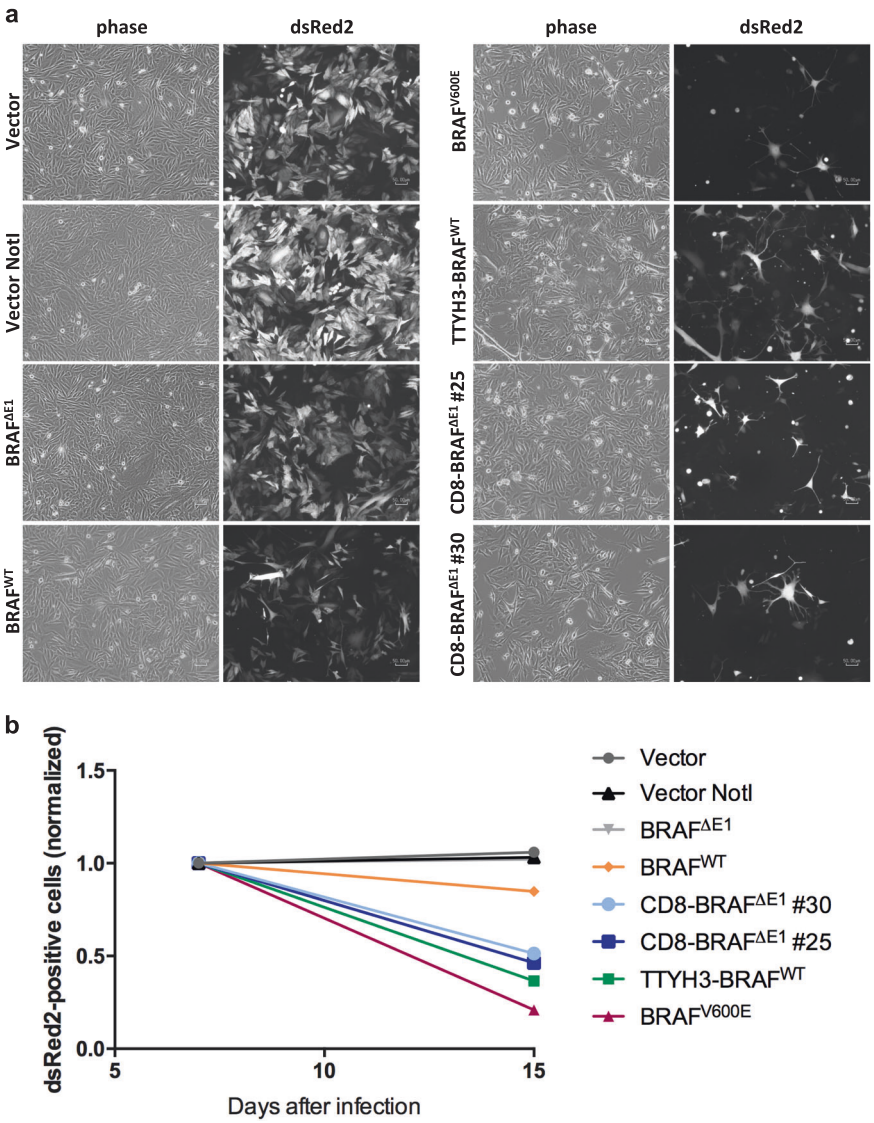

Fig. 6 TTYH3–BRAF^{WT} and other BRAF oncoproteins induce differentiation in LN-229ecoR cells. **a** LN-229ecoR cells were infected with the indicated pMIBerry constructs and infected cells were identified by their dsRed2 fluorescence ten days post infection. Note that expression of the transforming BRAF^{V600E}, TTYH3–BRAF^{WT}, and CD8–BRAF$^{\Delta E1}$ (two independently generated plasmid clones 25 and 30) induces a neuron like morphology, while cells infected with the control vectors or those expressing BRAF^{WT} maintain their morphology. The pMIBerry NotI vector differs from the parental pMIBerry vector only by the absence of the second NotI restriction site. Data are representative of two independent infections. **b** Flow cytometric assessment of the abundance of dsRed2 expressing cells seven and 15 days post infection. The percentage of dsRed2 positive cells at day 7 was arbitrarily set to 1

biochemical and pharmacological experiments. In contrast, GSC-233ecoR cells appeared more robust to ectopic BRAF expression, and hence appeared more suitable for such analyses (Supplementary Fig. S7b).

Drug sensitivity of TTYH3–BRAF^{WT}-mediated signaling

Next, we assayed the effects of (pre)clinically relevant RAF and MEK inhibitors to identify strategies for treating tumors driven by such unusual BRAF fusion proteins. Initially, we screened various RAF inhibitors in Plat-E cells ectopically expressing the BRAF proteins in question. Given the resistance of non-V600E BRAF oncoproteins toward vemurafenib, in particular splice variants and fusion proteins with prominent dimerization behavior [14], we chose dabrafenib and trametinib as these compounds can be safely combined [15] and as dabrafenib has been hardly explored in the context of BRAF fusion proteins. In addition, we tested whether the paradox-breaking dual pan-RAF/SRC family inhibitor CCT196969 [55] and the paradox-breaking vemurafenib derivatives PLX7904 and PLX8394 [56] would affect TTYH3–BRAF^{WT}-induced MEK/ERK phosphorylation.

As shown in Supplementary Fig. S8a, b, both dabrafenib and CCT196969 reduced MEK/ERK phosphorylation elicited by TTYH3–BRAF^{WT}, albeit only at higher and clinically irrelevant doses such as 5 and 10 µM dabrafenib. In contrast, MEK phosphorylation, the most direct assessment of cellular RAF activity, was clearly affected by 1 µM dabrafenib and CCT196969 in BRAF^{V600E}-overexpressing cells. It should be kept in mind that, due to the lack of a cell line with an endogenous *TTYH3–BRAF* fusion, we were forced to apply an ectopic overexpression approach.

Consequently, the observed drug efficacies, as judged by the absolute molarities at which full inhibition of MEK and ERK phosphorylation was observed, might differ in our cell line models from those with endogenous $BRAF^{V600E}$ mutations. Moreover, as also observed in other cell types [57], even with endogenous $BRAF^{V600E}$ mutations [58], we observed that the reduction of ERK phosphorylation levels lagged behind that of MEK phosphorylation. This could be explained by the drug-induced loss of ERK phosphatases such as DUSP6 and other negative feedback loops that maintain ERK phosphorylation via rheostasis despite a reduction of input signals [57–59]. Therefore, the degree of phospho-MEK reduction is more informative in assessing the action of RAF inhibitors.

As shown in Supplementary Figs. S8c and S9a, the pan-RAF and multikinase inhibitor sorafenib effectively suppressed MEK and ERK phosphorylation elicited by TTYH3–$BRAF^{WT}$ at 5 and 10 µM, concentrations that were observed in human plasma [60, 61]. Given this response, we decided to test sorafenib in GSC-233ecoR cells (Fig. 7a). Again, 5 µM sorafenib suppressed MEK phosphorylation by more than 75%, while it had little impact on $BRAF^{V600E}$, as expected from its well-known type II binding mode [15]. Similarly, sorafenib, albeit used at the higher but clinically still relevant concentration of 10 µM [61], blocked MEK/ERK phosphorylation in the NHA/TAg/ecoR lysates used for the co-immunoprecipitation assay (Supplementary Fig. S5b).

Classic RAF fusions including only the CR3 trigger ERK pathway activation, and this feature has been used as an indication for MEK inhibitors, leading to tumor responses [2, 20, 62–65]. Indeed, the MEK inhibitor trametinib suppressed ERK and, to a lesser extent, MEK phosphorylation in GSC-233 and Plat-E cells (Fig. 7b and Supplementary Fig. S9b). The effect of trametinib on both phosphorylation events can be explained by the so-called 'feedback buster' property of trametinib that, in addition to its action as an ATP-competitive inhibitor, impairs the phosphorylation of a critical MEK1/2 AL site by activated RAF [66].

Next, we tested the paradox breakers PLX7904 and PLX8394 for their efficacy to inhibit the MEK phosphorylation potential of TTYH3–$BRAF^{WT}$ and $BRAF^{V600E}$. These compounds have only been tested in the context of typical BRAF fusion proteins, such as KIAA1549–BRAF, or vemurafenib-promoted BRAF splice variants, both carrying mainly the CR3 as BRAF component [14, 67]. Therefore, it was of interest whether these drugs could reduce the activity of TTYH3–$BRAF^{WT}$. Indeed, both paradox breakers suppressed the high MEK phosphorylation elicited by $BRAF^{V600E}$ at 0.3 µM, while those triggered by TTYH3–$BRAF^{WT}$ showed a lesser differential at this concentration (Fig. 7c and Supplementary Fig. S10). Ten times higher drug concentrations, however, also reduced MEK phosphorylation in TTYH3–$BRAF^{WT}$- expressing cells by more than 70% and showed similar efficacy as 5 µM sorafenib. This data is consistent with the western blot by Yao et al. showing the effect of PLX8394 on KIAA1549–BRAF-expressing HEK293 cells [67], suggesting that both BRAF fusions, despite their structural differences (Fig. 1e), do not significantly differ in PLX8394 sensitivity. It should be noted that a direct comparison of the MEK phosphorylation potentials of $BRAF^{V600E}$ and TTYH3–$BRAF^{WT}$ is complicated by the lower expression of the latter. However, by comparing the phospho-MEK signals in $BRAF^{V600E}$ and TTYH3–$BRAF^{WT}$-infected GBM cells, it is obvious that these paradox breakers appear more effective against $BRAF^{V600E}$, as they, despite the abundance of the oncoprotein, achieve a reduction in MEK phosphorylation by 96 and 99% at 0.3 and 3 µM, respectively.

No evidence for collaboration between TTYH3–$BRAF^{WT}$ and PIK3R1 mutations

Mutations in the PI3K/AKT/mTOR pathway frequently occur in GBM and sometimes coexist with RAS/ERK axis alterations such as *NF1* loss [29]. Given that both pathways collaborate in the progression of various tumour entities, as exemplified by $BRAF^{V600E}$ driven melanoma and GBM mouse models [68, 69], we asked whether the poorly characterized $PIK3R1^{G376R}$ allele and the novel $PIK3R1^{H407Q}$ mutant, which were identified in the GBM patient (Supplementary Table S1), possess oncogenic potential, either alone or in combination with TTYH3–$BRAF^{WT}$. First, we tested whether both mutants can confer interleukin-3 (IL3) independence in Ba/F3 cells, a well-established model system to gauge the transforming potential of *PIK3R1* mutants [70, 71]. As shown in Supplementary Fig. S11a, b, however, both mutants were unable to drive Ba/F3 survival in the absence of IL3. This data is in line with two previous studies reporting only very weak signalling and transforming potential of $PIK3R1^{G376R}$ [70, 72] and further suggests that $PIK3R1^{H407Q}$ might be a passenger mutant.

Previously, we observed that high activity BRAF mutants such as $BRAF^{V600E}$ or $BRAF^{insT}$ induce cell cycle arrest and an elongated morphology in parental NHA cells [73]. This phenotype is preserved in their NHA/Tag/ecoR derivative (Supplementary Fig. S11c), suggesting that chronic ERK activation rather impedes cell cycle progression in these cells and requires the cooperation with other pathways to drive proliferation. Therefore, we generated NHA/Tag/ecoR cells stably expressing the PIK3R1 proteins in question, subsequently infected them with expression vectors for TTYH3–$BRAF^{WT}$ or control constructs and monitored the abundance of dsRed2 expressing cells over time. While the percentage of dsRed2 positive control cells remained stable, the number of TTYH3–$BRAF^{WT}$

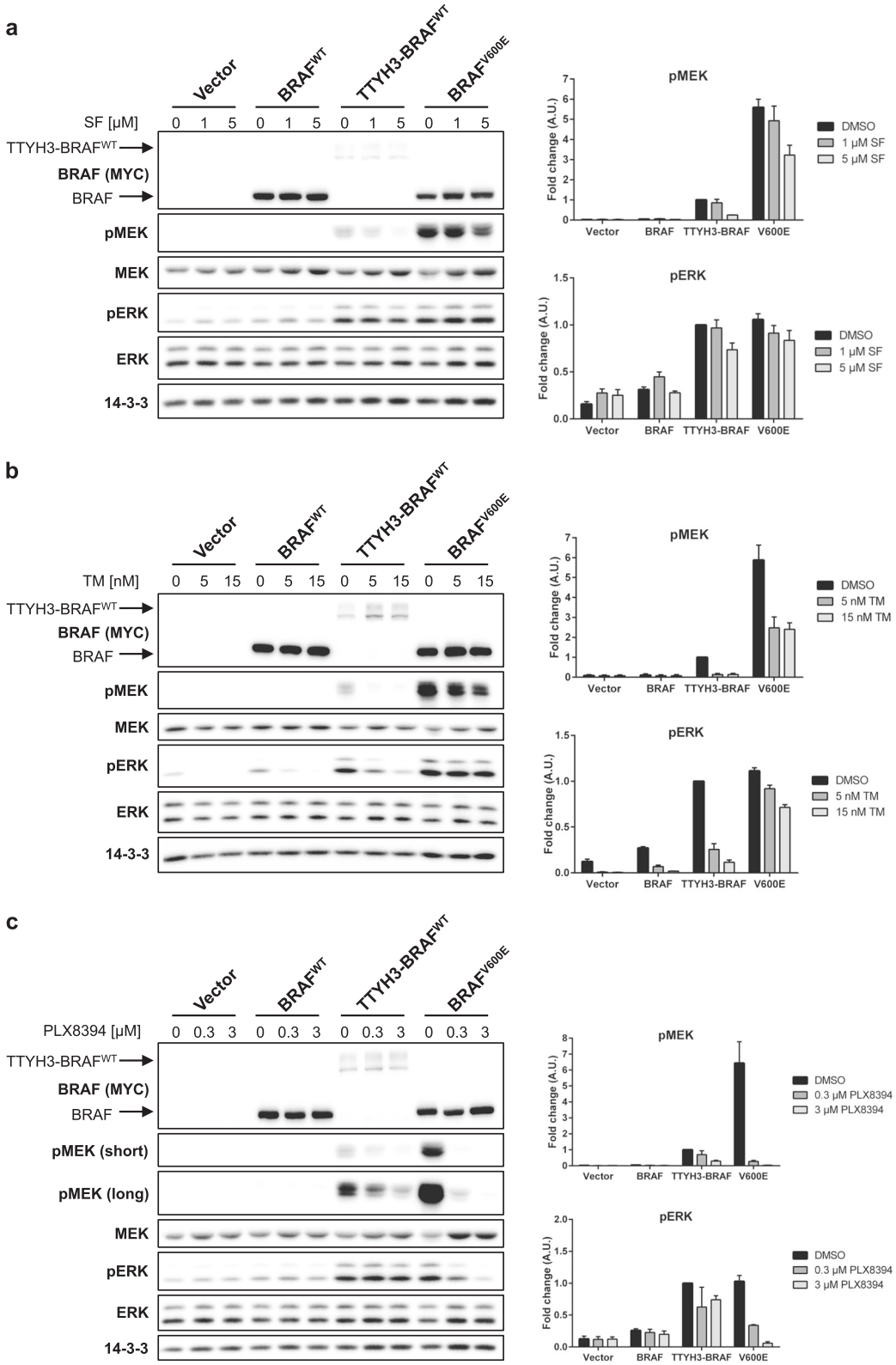

Fig. 7 TTYH3–BRAF^{WT} mediated signaling is susceptible to RAF and MEK inhibition in GSC-233ecoR GBM cells. GSC-233ecoR cells were infected with the indicated constructs and treated either with the indicated doses of **a** sorafenib, **b** trametinib, or **c** the paradox-breaker PLX8394 for 4 h. Shown are western blots of one out of three independent biological replicates using the indicated antibodies. Detection of 14–3–3 serves as an additional loading control. Shown on the right is the quantification of the pMEK and pERK signals normalized to the loading control ($n = 3$). TTYH3–BRAF^{WT} mediated pMEK and pERK signals in vehicle (DMSO) treated cells was arbitrarily set to 1. Shown is the mean ± S.E.M

expressing cells significantly decreased within 14 days (Supplementary Fig. S11d, e). Taken together, both assays did not reveal a discernible transforming activity of both *PIK3R1* mutants and do not support their collaboration with TTYH3–BRAF^{WT}.

Discussion

Here, we demonstrate that the TTYH3–BRAF^{WT} fusion protein identified in GBM represents a bona fide oncogenic driver whose downstream effects can be blocked by the pan-RAF/multikinase inhibitor sorafenib, BRAF paradox breakers, and the MEK inhibitor trametinib, thus providing an immediate therapeutic opportunity. Indeed, combination treatment with a MEK inhibitor could lower the risk of paradoxical ERK pathway activation by sorafenib monotherapy, which has been described in low-grade glioma patients [61]. Moreover, the discovery of TTYH3–BRAF^{WT} highlights the clinical value of exome or genome and RNA sequencing in individual cancer patients—even in diseases whose genomic landscape has been mapped such as GBM [28, 29]—as a more focused mutational analysis covering the *BRAF* hotspot exons 11 and 15 would have classified this tumor as "*BRAF* wildtype".

Our study also represents an example for "bidirectional translation" as the discovery of the TTYH3–BRAF^{WT} fusion has not only yielded potential treatment options, but also identified a novel mechanism of BRAF-mediated transformation. In sharp contrast to the oncogenic BRAF fusions identified so far [2, 19, 36], TTYH3–BRAF^{WT} retains all known critical autoinhibitory features. TTYH3–BRAF^{WT} only lacks amino acids encoded by exon 1, whose function remains ill-defined except for a contribution to dimerization [74]. Thus far, only two other BRAF fusion proteins have been reported that correspond to TTYH3–BRAF^{WT} in terms of their BRAF moiety. SND1–BRAF was observed in three lung adenocarcinoma samples and contains amino acids encoded by the first nine exons of *SND1* that are N-terminally linked to the polypeptide derived from *BRAF* exons 2 to 18 [75]. In AHCYL2–BRAF, observed in cutaneous melanoma, the same BRAF portion is fused to adenosylhomocysteinase like 2 [76]. In contrast to our assays with TTYH3–BRAF^{WT}, however, SND1–BRAF and AHCYL2–BRAF did not elicit significantly elevated MEK/ERK phosphorylation compared with BRAF^{WT} upon ectopic expression [75, 76]. Although we did not directly compare TTYH3–BRAF^{WT}, SND1–BRAF, and AHCYL2–BRAF, our data suggest that TTYH3–BRAF^{WT} is a far more potent oncoprotein due to the presence of the TTYH3 moiety. Indeed, while SND1, as member of the RISC complex [75], and AHCYL2 are both located in the cytoplasm, TTYH proteins are embedded in the endomembrane system and the plasma membrane [33]. This implies that tethering of an otherwise autoinhibited BRAF protein to the (endo)membrane system represents the pathogenic mechanism underlying the oncogenic potential of TTYH3–BRAF^{WT} (Fig. 4c). Our concept is supported by our synthetic approach, in which we demonstrated that fusion of the autoinhibited BRAF$^{\Delta E1}$ component of TTYH3–BRAF^{WT} to CD8 generates a strong MEK/ERK activator and transforming protein. The pathomechanism of TTYH3–BRAF^{WT} ties in with previous experiments, in which artificial membrane tethering of full-length BRAF or RAF1 by fusing their C-termini to the polybasic region and CAAX box of KRAS was sufficient to generate an oncoprotein [11, 77, 78]. However, TTYH3–BRAF^{WT} differs from BRAF^{CAAX} as it is tethered to the membrane via its N-terminal end and thus represents the first membrane-associated near-full-length BRAF protein described in tumors (Fig. 8). Because BRAF$^{\Delta E1}$ behaves like BRAF^{WT}, our study identifies TTYH3–BRAF^{WT} as the first BRAF fusion whose oncogenic potential is clearly defined by the fusion partner and not the primary structure of the BRAF moiety. In the present work, we have also obtained new insights into the localization of TTYH3, which had not been investigated for this family member. Like TTYH1 and TTYH2, TTYH3 and the TTYH3–BRAF fusion protein localize to membranes and were concentrated in vesicular structures and in the Golgi apparatus area. Our data on TTYH3–BRAF^{WT} and CD8–BRAF$^{\Delta E1}$, which also strongly localizes to the endomembrane system, further supports the concept that MEK/ERK signals can originate from the endomembrane system [79]. This finding could be relevant for the interpretation of other tumor-associated RAF fusion proteins and highlights the necessity to consider the biology of the fusion partner as it has been recently demonstrated for the QKI–RAF1 fusion [20].

The various BRAF oncoproteins differ in terms of their precise mechanism of oncogenic activation and hence their dependence on positive and negative regulatory processes [3, 8, 11]. We therefore dissected the signaling requirements of TTYH3–BRAF^{WT}. Interestingly, TTYH3–BRAF^{R188L} was still able to transform MEFs and displayed a high MEK/ERK activation potential, suggesting that membrane tethering alleviates the necessity for BRAF activation by RAS. The oncogenic properties and RAS independence of TTYH3–BRAF^{WT}, BRAF–CAAX, and RAF1–CAAX raise the question why membrane tethering confers transforming potential to RAF. One possibility is that, maybe supported by protein–lipid interactions, membrane-tethered RAF kinases are more likely to exist in an open conformation, which in turn facilitates the dimerization and subsequent allosteric transactivation of the exposed kinase domains.

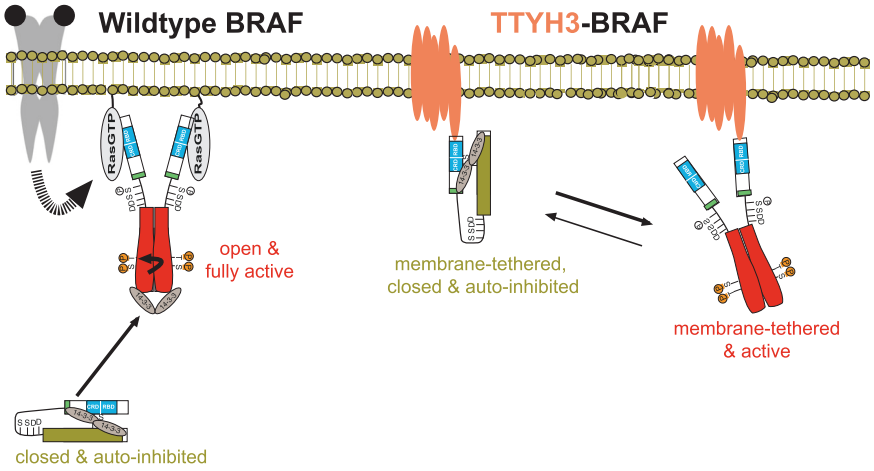

Fig. 8 Model illustrating how TTYH3–BRAF overcomes BRAF autoinhibition. See discussion for further details

Thus, membrane-tethered RAF kinases are not fully active per se, but are primed for full activation by mechanisms that would only occur in the activation of wild-type RAF kinases following RAS-mediated membrane recruitment. Indeed, we show that the elevated MEK/ERK phosphorylation potential of TTYH3–BRAF^{WT} requires critical structural prerequisites that are involved in BRAF activation following RAS binding, such as the AL phosphorylation sites T599 and S602 and an intact DIF. Thus, TTYH3–BRAF^{WT} displays similar regulatory requirements as typical BRAF fusion proteins lacking the autoinhibitory moiety, e.g., FAM131B–BRAF and KIAA1549–BRAF, and various non-V600E full-length BRAF oncoproteins [8, 11, 14, 16, 41]. In terms of their dimerization behavior, BRAF fusion proteins are usually considered as homodimers. However, we now show that TTYH3–BRAF^{WT} forms both RAF homo- and heterodimers and that the presence of the DIF residue R509 is required for its ability to induce MEK phosphorylation. R509 plays a versatile role in RAF signaling. First, it fulfills an important, albeit nonessential role in dimer formation, although its histidine substitution differently impacts on homo- vs. heterodimer formation and/or stability as judged by co-immunoprecipitation assays [8]. This finding could be explained by very recent insights into the structures of BRAF homo- and BRAF/RAF1 heterodimers that are also relevant for our understanding of the drug selectivity of RAF complexes [67]. Future studies will address whether the TTYH3 partner, which, as a VRAC component [31], might form higher ordered complexes on its own, modulates the dimerization potential and partner choice, i.e., formation of homo- vs. heterodimers, of the BRAF$^{\Delta E1}$ moiety. Second and most importantly, R509 plays an essential role in allosteric transactivation [5, 8–10] and is hence critical for the transforming potential of most BRAF oncoproteins. The dependence of TTYH3–BRAF^{WT} (this study) and of typical BRAF fusions on an intact DIF [14] highlights the possibility that yet-to-be-developed compounds that prevent dimerization or processes promoting it, e.g., AL phosphorylation (see Ref. [11]. and references therein for discussion), could be effective in targeting BRAF fusion proteins. Such compounds could be even superior to ATP-competitive inhibitors that, at least those in clinical use, fail to inhibit BRAF fusion proteins due to their high dimerization potential and the associated phenomenon of negative cooperativity [14, 16, 67].

Materials and methods

Patient samples

For WES, a fresh-frozen tumor specimen and a matched blood sample were collected from a patient who had been diagnosed with GBM multiforme according to World Health Organization criteria. Samples were pseudonymized, and tumor histology and cellularity were assessed at the Institute of Pathology, Heidelberg University Hospital, prior to further processing. The patient provided written informed consent under an institutional review board-approved protocol, and the study was conducted in accordance with the Declaration of Helsinki.

Immunohistochemistry

Immunohistochemistry was performed using a 1:100 dilution of anti-pERK antibody from Cell Signaling Technology (#9101) as described previously [80].

Cultivation and treatment of cells

The culture of non-GBM cell lines, their transfection, as well as the in-house generation, and culture of immortalized

Braf$^{floxE12/floxE12}$ MEFs were described previously [8, 41]. Plat-E cells were provided from Dr Kitamura (University of Tokyo). NHA/TAg/ecoR were generated in-house from normal human astrocytes (Lonza) as described previously [40]. The GBM cell lines LN-229 and GSC-233 cells and their derivatives were cultivated in DMEM (4.5 g/l glucose, 10% fetal calf serum, 2 mM L-glutamine, 10 mM HEPES, 200 U/ml penicillin, 200 µg/ml streptomycin). Cells tested negative for *Mycoplasma* (Eurofins, Cologne) and the 100% identity of LN-229 cells was confirmed by single nucleotide polymorphism (SNP)-profiling (Multiplexion, Heidelberg). As expected, the recently established GSC-233 line [51] showed a unique SNP profile, unrelated to any of the 900 authenticated cell lines in the Multiplexion database. Details on viral transduction are provided in Supplementary Information. Vemurafenib, dabrafenib, trametinib, sorafenib, and the paradox breakers PLX7904 and PLX8394 were obtained from SelleckChem. CCT196969 was purchased from Reagency. All inhibitors were dissolved in DMSO.

Western blotting

These methods have been described in detail previously [8, 58]. In brief, lysates were size separated by 10% SDS-PAGE followed by transfer to PVDF membranes and proteins of interest were detected with the following primary antibodies: anti-MEK1/2 (#9122), anti-phospho-MEK1/2 (#9121), anti-ERK1/2 (#9102), anti-phospho-ERK1/2 (#9101), anti-MYC 9B11 (#2276) (all from Cell Signaling), anti-HA 3F10 (#11867431001) (Roche), anti-B-Raf F7 (#sc-5284), anti-Raf-1 C-12 (#sc-133), anti-A-Raf (#sc-408) anti-14–3–3 (#sc-1657) (all from Santa Cruz Biotechnology), and anti-FLAG M2 (F1804; Sigma-Aldrich). Bound primary antibodies were detected using HRP-labelled secondary antibodies and a PeqlabTM Fusion Solo device. Recorded signals were quantified using Fusion software (version 16.08).

Quantification and statistical analysis

Quantitative data are presented as mean ± SEM of three independent biological replicates. Multiple group comparisons were performed by two-way ANOVA Fisher LSD test using GraphPad Prism 6. A p-value of ≤0.05 was considered statistically significant.

Acknowledgements This work was supported by the German Research Foundation (DFG) by BR3662/4–1, SFB 850 B04, and EXC 294 *BIOSS* to TB, and by grant 021 from the DKFZ-Heidelberg Center for Personalized Oncology to HG and SF, TB is the recipient of a Heisenberg Professorship from the DFG. CS is supported in part by the DFG-funded Spemann Graduate School of Biology and Medicine (SGBM, GSC 4). We thank the DKFZ-HIPO Sample Processing Laboratory, the DKFZ Genomics and Proteomics Core Facility, the Omics IT and Data Management Core Facility for technical support. We also thank D. Richter, K. Beck, K. Willmund, R. Eils, and P. Lichter for infrastructure and program development within DKFZ-HIPO.

Author contribution FW, RH, SB, CS, MI, VH, and TB performed all wet lab experiments. MF, MR, GW, BH, SU, BB, SF, and TB analyzed the complex rearrangements of the *TTYH3* and *BRAF* loci. CH, PH, SK, ON, DR, CvK, WW, AS, HG, and SF collected and analyzed clinical data. DHH provided GBM cell lines and important scientific input. FW, SF, and TB conceived the project and wrote the paper with MF.

Compliance with ethical standards

Conflict of interest The authors declare that they have no conflict of interest.

Publisher's note Springer Nature remains neutral with regard to jurisdictional claims in published maps and institutional affiliations.

References

1. Turski ML, Vidwans SJ, Janku F, Garrido-Laguna I, Munoz J, Schwab R, et al. Genomically driven tumors and actionability across histologies: BRAF-mutant cancers as a paradigm. Mol Cancer Ther. 2016;15:533–47.
2. Ross JS, Wang K, Chmielecki J, Gay L, Johnson A, Chudnovsky J, et al. The distribution of BRAF gene fusions in solid tumors and response to targeted therapy. Int J Cancer. 2016;138:881–90.
3. Dankner M, Rose AAN, Rajkumar S, Siegel PM, Watson IR. Classifying BRAF alterations in cancer: new rational therapeutic strategies for actionable mutations. Oncogene. 2018;37:3183–99.
4. Chen SH, Zhang Y, Van Horn RD, Yin T, Buchanan S, Yadav V, et al. Oncogenic BRAF deletions that function as homodimers and are sensitive to inhibition by RAF dimer inhibitor LY3009120. Cancer Discov. 2016;6:300–15.
5. Lavoie H, Therrien M. Regulation of RAF protein kinases in ERK signalling. Nat Rev Mol Cell Biol. 2015;16:281–98.
6. Terrell EM, Morrison DK. Ras-mediated activation of the Raf family kinases. Cold Spring Harb Perspect Med. 2019;9. pii: a033746. https://doi.org/10.1101/cshperspect.a033746.
7. Eisenhardt AE, Sprenger A, Roring M, Herr R, Weinberg F, Kohler M, et al. Phospho-proteomic analyses of B-Raf protein complexes reveal new regulatory principles. Oncotarget. 2016;7:26628–52.
8. Röring M, Herr R, Fiala GJ, Heilmann K, Braun S, Eisenhardt AE, et al. Distinct requirement for an intact dimer interface in wild-type, V600E and kinase-dead B-Raf signalling. EMBO J. 2012;31:2629–47.
9. Freeman AK, Ritt DA, Morrison DK. Effects of Raf dimerization and its inhibition on normal and disease-associated Raf signaling. Mol Cell. 2013;49:751–8.
10. Hu J, Stites EC, Yu H, Germino EA, Meharena HS, Stork PJ, et al. Allosteric activation of functionally asymmetric RAF kinase dimers. Cell. 2013;154:1036–46.
11. Köhler M, Röring M, Schorch B, Heilmann K, Stickel N, Fiala GJ, et al. Activation loop phosphorylation regulates B-Raf in vivo and transformation by B-Raf mutants. EMBO J. 2016;35:143–61.
12. Diedrich B, Rigbolt KT, Roring M, Herr R, Kaeser-Pebernard S, Gretzmeier C, et al. Discrete cytosolic macromolecular BRAF complexes exhibit distinct activities and composition. EMBO J. 2017;36:646–63.

13. Yuan J, Ng WH, Lam PYP, Wang Y, Xia H, Yap J, et al. The dimer-dependent catalytic activity of RAF family kinases is revealed through characterizing their oncogenic mutants. Oncogene. 2018;37:5719–34.
14. Sievert AJ, Lang SS, Boucher KL, Madsen PJ, Slaunwhite E, Choudhari N, et al. Paradoxical activation and RAF inhibitor resistance of BRAF protein kinase fusions characterizing pediatric astrocytomas. Proc Natl Acad Sci USA. 2013;110:5957–62.
15. Karoulia Z, Gavathiotis E, Poulikakos PI. New perspectives for targeting RAF kinase in human cancer. Nat Rev Cancer. 2017;17:676–91.
16. Yao Z, Torres NM, Tao A, Gao Y, Luo L, Li Q, et al. BRAF mutants evade ERK-dependent feedback by different mechanisms that determine their sensitivity to pharmacologic inhibition. Cancer Cell. 2015;28:370–83.
17. Palanisamy N, Ateeq B, Kalyana-Sundaram S, Pflueger D, Ramnarayanan K, Shankar S, et al. Rearrangements of the RAF kinase pathway in prostate cancer, gastric cancer and melanoma. Nat Med. 2010;16:793–8.
18. Jones DT, Kocialkowski S, Liu L, Pearson DM, Ichimura K, Collins VP. Oncogenic RAF1 rearrangement and a novel BRAF mutation as alternatives to KIAA1549:BRAF fusion in activating the MAPK pathway in pilocytic astrocytoma. Oncogene. 2009;28:2119–23.
19. Cin H, Meyer C, Herr R, Janzarik WG, Lambert S, Jones DT, et al. Oncogenic FAM131B-BRAF fusion resulting from 7q34 deletion comprises an alternative mechanism of MAPK pathway activation in pilocytic astrocytoma. Acta Neuropathol. 2011;121:763–74.
20. Jain P, Fierst TM, Han HJ, Smith TE, Vakil A, Storm PB, et al. CRAF gene fusions in pediatric low-grade gliomas define a distinct drug response based on dimerization profiles. Oncogene. 2017;36:6348–58.
21. Jones DT, Kocialkowski S, Liu L, Pearson DM, Backlund LM, Ichimura K, et al. Tandem duplication producing a novel oncogenic BRAF fusion gene defines the majority of pilocytic astrocytomas. Cancer Res. 2008;68:8673–7.
22. Selt F, Hohloch J, Hielscher T, Sahm F, Capper D, Korshunov A, et al. Establishment and application of a novel patient-derived KIAA1549:BRAF-driven pediatric pilocytic astrocytoma model for preclinical drug testing. Oncotarget. 2017;8:11460–79.
23. Tien AC, Tsai HH, Molofsky AV, McMahon M, Foo LC, Kaul A, et al. Regulated temporal-spatial astrocyte precursor cell proliferation involves BRAF signalling in mammalian spinal cord. Development. 2012;139:2477–87.
24. Galabova-Kovacs G, Catalanotti F, Matzen D, Reyes GX, Zezula J, Herbst R, et al. Essential role of B-Raf in oligodendrocyte maturation and myelination during postnatal central nervous system development. J Cell Biol. 2008;180:947–55.
25. Berghoff AS, Preusser M. BRAF alterations in brain tumours: molecular pathology and therapeutic opportunities. Curr Opin Neurol. 2014;27:689–96.
26. Behling F, Schittenhelm J. Oncogenic BRAF alterations and their role in brain tumors. Cancers (Basel). 2019;11. pii: E794. https://doi.org/10.3390/cancers11060794.
27. Horak P, Klink B, Heining C, Groschel S, Hutter B, Frohlich M, et al. Precision oncology based on omics data: the NCT Heidelberg experience. Int J Cancer. 2017;141:877–86.
28. Frattini V, Trifonov V, Chan JM, Castano A, Lia M, Abate F, et al. The integrated landscape of driver genomic alterations in glioblastoma. Nat Genet. 2013;45:1141–9.
29. Brennan CW, Verhaak RG, McKenna A, Campos B, Noushmehr H, Salama SR, et al. The somatic genomic landscape of glioblastoma. Cell. 2013;155:462–77.
30. Suzuki M, Mizuno A. A novel human Cl(-) channel family related to Drosophila flightless locus. J Biol Chem. 2004;279:22461–8.
31. Han YE, Kwon J, Won J, An H, Jang MW, Woo J, et al. Tweety-homolog (Ttyh) family encodes the pore-forming subunits of the swelling-dependent volume-regulated Anion channel (VRACs-well) in the brain. Exp Neurobiol. 2019;28:183–215.
32. He Y, Hryciw DH, Carroll ML, Myers SA, Whitbread AK, Kumar S, et al. The ubiquitin-protein ligase Nedd4-2 differentially interacts with and regulates members of the Tweety family of chloride ion channels. J Biol Chem. 2008;283:24000–10.
33. He Y, Ramsay AJ, Hunt ML, Whitbread AK, Myers SA, Hooper JD. N-glycosylation analysis of the human Tweety family of putative chloride ion channels supports a penta-spanning membrane arrangement: impact of N-glycosylation on cellular processing of Tweety homologue 2 (TTYH2). Biochem J. 2008;412:45–55.
34. Mercer KE, Pritchard CA. Raf proteins and cancer: B-Raf is identified as a mutational target. Biochim Biophys Acta. 2003;1653:25–40.
35. Chmielecki J, Hutchinson KE, Frampton GM, Chalmers ZR, Johnson A, Shi C, et al. Comprehensive genomic profiling of pancreatic acinar cell carcinomas identifies recurrent RAF fusions and frequent inactivation of DNA repair genes. Cancer Discov. 2014;4:1398–405.
36. Hutchinson KE, Lipson D, Stephens PJ, Otto G, Lehmann BD, Lyle PL, et al. BRAF fusions define a distinct molecular subset of melanomas with potential sensitivity to MEK inhibition. Clin Cancer Res. 2013;19:6696–702.
37. Nicolaides TP, Li H, Solomon DA, Hariono S, Hashizume R, Barkovich K, et al. Targeted therapy for BRAFV600E malignant astrocytoma. Clin Cancer Res. 2011;17:7595–604.
38. Jung E, Osswald M, Blaes J, Wiestler B, Sahm F, Schmenger T, et al. Tweety-homolog 1 drives brain colonization of gliomas. J Neurosci. 2017;37:6837–50.
39. Stefaniuk M, Swiech L, Dzwonek J, Lukasiuk K. Expression of Ttyh1, a member of the Tweety family in neurons in vitro and in vivo and its potential role in brain pathology. J Neurochem. 2010;115:1183–94.
40. International Cancer Genome Consortium PedBrain Tumor P. Recurrent MET fusion genes represent a drug target in pediatric glioblastoma. Nat Med. 2016;22:1314–20.
41. Kordes M, Röring M, Heining C, Braun S, Hutter B, Richter D, et al. Cooperation of BRAF(F595L) and mutant HRAS in histiocytic sarcoma provides new insights into oncogenic BRAF signaling. Leukemia. 2016;30:937–46.
42. Poulikakos PI, Persaud Y, Janakiraman M, Kong X, Ng C, Moriceau G, et al. RAF inhibitor resistance is mediated by dimerization of aberrantly spliced BRAF(V600E). Nature. 2011;480:387–90.
43. Heidorn SJ, Milagre C, Whittaker S, Nourry A, Niculescu-Duvas I, Dhomen N, et al. Kinase-dead BRAF and oncogenic RAS cooperate to drive tumor progression through CRAF. Cell. 2010;140:209–21.
44. Rushworth LK, Hindley AD, O'Neill E, Kolch W. Regulation and role of Raf-1/B-Raf heterodimerization. Mol Cell Biol. 2006;26:2262–72.
45. Ritt DA, Monson DM, Specht SI, Morrison DK. Impact of feedback phosphorylation and Raf heterodimerization on normal and mutant B-Raf signaling. Mol Cell Biol. 2010;30:806–19.
46. Littman DR, Thomas Y, Maddon PJ, Chess L, Axel R. The isolation and sequence of the gene encoding T8: a molecule defining functional classes of T lymphocytes. Cell. 1985;40:237–46.
47. Hennecke S, Cosson P. Role of transmembrane domains in assembly and intracellular transport of the CD8 molecule. J Biol Chem. 1993;268:26607–12.
48. Iodice L, Sarnataro S, Bonatti S. The carboxyl-terminal valine is required for transport of glycoprotein CD8 alpha from the endoplasmic reticulum to the intermediate compartment. J Biol Chem. 2001;276:28920–6.

49. Ramis G, Thomas-Moya E, Fernandez de Mattos S, Rodriguez J, Villalonga P. EGFR inhibition in glioma cells modulates Rho signaling to inhibit cell motility and invasion and cooperates with temozolomide to reduce cell growth. PLoS One. 2012;7:e38770.
50. Fan QW, Cheng CK, Gustafson WC, Charron E, Zipper P, Wong RA, et al. EGFR phosphorylates tumor-derived EGFRvIII driving STAT3/5 and progression in glioblastoma. Cancer Cell. 2013;24:438–49.
51. Ricklefs FL, Maire CL, Reimer R, Duhrsen L, Kolbe K, Holz M, et al. Imaging flow cytometry facilitates multiparametric characterization of extracellular vesicles in malignant brain tumours. J Extracell Vesicles. 2019;8:1588555.
52. Marshall CJ. Specificity of receptor tyrosine kinase signaling: transient versus sustained extracellular signal-regulated kinase activation. Cell. 1995;80:179–85.
53. Masilamani AP, Ferrarese R, Kling E, Thudi NK, Kim H, Scholtens DM, et al. KLF6 depletion promotes NF-kappaB signaling in glioblastoma. Oncogene. 2017;36:3562–75.
54. Aoki Y, Niihori T, Narumi Y, Kure S, Matsubara Y. The RAS/MAPK syndromes: novel roles of the RAS pathway in human genetic disorders. Hum Mutat. 2008;29:992–1006.
55. Girotti MR, Lopes F, Preece N, Niculescu-Duvaz D, Zambon A, Davies L, et al. Paradox-breaking RAF inhibitors that also target SRC are effective in drug-resistant BRAF mutant melanoma. Cancer Cell. 2015;27:85–96.
56. Zhang C, Spevak W, Zhang Y, Burton EA, Ma Y, Habets G, et al. RAF inhibitors that evade paradoxical MAPK pathway activation. Nature. 2015;526:583–6.
57. Phuchareon J, McCormick F, Eisele DW, Tetsu O. EGFR inhibition evokes innate drug resistance in lung cancer cells by preventing Akt activity and thus inactivating Ets-1 function. Proc Natl Acad Sci USA. 2015;112:E3855–3863.
58. Herr R, Halbach S, Heizmann M, Busch H, Boerries M, Brummer T. BRAF inhibition upregulates a variety of receptor tyrosine kinases and their downstream effector Gab2 in colorectal cancer cell lines. Oncogene. 2018;37:1576–93.
59. Pratilas CA, Taylor BS, Ye Q, Viale A, Sander C, Solit DB, et al. (V600E)BRAF is associated with disabled feedback inhibition of RAF-MEK signaling and elevated transcriptional output of the pathway. Proc Natl Acad Sci USA. 2009;106:4519–24.
60. Strumberg D, Richly H, Hilger RA, Schleucher N, Korfee S, Tewes M, et al. Phase I clinical and pharmacokinetic study of the Novel Raf kinase and vascular endothelial growth factor receptor inhibitor BAY 43-9006 in patients with advanced refractory solid tumors. J Clin Oncol. 2005;23:965–72.
61. Karajannis MA, Legault G, Fisher MJ, Milla SS, Cohen KJ, Wisoff JH, et al. Phase II study of sorafenib in children with recurrent or progressive low-grade astrocytomas. Neuro Oncol. 2014;16:1408–16.
62. Isaacson AL, Guseva NV, Bossler AD, Ma D. Urothelial carcinoma with an NRF1-BRAF rearrangement and response to targeted therapy. Cold Spring Harb Mol Case Stud. 2019;5. pii: a003848. https://doi.org/10.1101/mcs.a003848.
63. Fangusaro J, Onar-Thomas A, Young Poussaint T, Wu S, Ligon AH, Lindeman N, et al. Selumetinib in paediatric patients with BRAF-aberrant or neurofibromatosis type 1-associated recurrent, refractory, or progressive low-grade glioma: a multicentre, phase 2 trial. Lancet Oncol. 2019;20:1011–22.
64. Kim HS, Jung M, Kang HN, Kim H, Park CW, Kim SM, et al. Oncogenic BRAF fusions in mucosal melanomas activate the MAPK pathway and are sensitive to MEK/PI3K inhibition or MEK/CDK4/6 inhibition. Oncogene. 2017;36:3334–45.
65. McEvoy CR, Xu H, Smith K, Etemadmoghadam D, San Leong H, Choong DY. et al. Profound MEK inhibitor response in a cutaneous melanoma harboring a GOLGA4-RAF1 fusion. J Clin Investig. 2019;129:1940–5.
66. Caunt CJ, Sale MJ, Smith PD, Cook SJ. MEK1 and MEK2 inhibitors and cancer therapy: the long and winding road. Nat Rev Cancer. 2015;15:577–92.
67. Yao Z, Gao Y, Su W, Yaeger R, Tao J, Na N, et al. RAF inhibitor PLX8394 selectively disrupts BRAF dimers and RAS-independent BRAF-mutant-driven signaling. Nat Med. 2019;25:284–91.
68. Dankort D, Curley DP, Cartlidge RA, Nelson B, Karnezis AN, Damsky WE Jr., et al. Braf(V600E) cooperates with Pten loss to induce metastatic melanoma. Nat Genet. 2009;41:544–52.
69. Robinson JP, VanBrocklin MW, Guilbeault AR, Signorelli DL, Brandner S, Holmen SL. Activated BRAF induces gliomas in mice when combined with Ink4a/Arf loss or Akt activation. Oncogene. 2010;29:335–44.
70. Zhang Y, Kwok-Shing NgP, Kucherlapati M, Chen F, Liu Y, Tsang YH, et al. A pan-cancer proteogenomic atlas of PI3K/AKT/mTOR pathway alterations. Cancer Cell. 2017;31:820–32 e823.
71. Ng PK, Li J, Jeong KJ, Shao S, Chen H, Tsang YH, et al. Systematic functional annotation of somatic mutations in cancer. Cancer Cell. 2018;33:450–62 e410.
72. Sun M, Hillmann P, Hofmann BT, Hart JR, Vogt PK. Cancer-derived mutations in the regulatory subunit p85alpha of phosphoinositide 3-kinase function through the catalytic subunit p110alpha. Proc Natl Acad Sci USA. 2010;107:15547–52.
73. Eisenhardt AE, Olbrich H, Roring M, Janzarik W, Anh TN, Cin H, et al. Functional characterization of a BRAF insertion mutant associated with pilocytic astrocytoma. Int J Cancer. 2011;129:2297–303.
74. Terai K, Matsuda M. The amino-terminal B-Raf-specific region mediates calcium-dependent homo- and hetero-dimerization of Raf. Embo J. 2006;25:3556–64.
75. Jang JS, Lee A, Li J, Liyanage H, Yang Y, Guo L, et al. Common oncogene mutations and novel SND1-BRAF transcript fusion in lung adenocarcinoma from never smokers. Sci Rep. 2015;5:9755.
76. Lu H, Villafane N, Dogruluk T, Grzeskowiak CL, Kong K, Tsang YH, et al. Engineering and functional characterization of fusion genes identifies novel oncogenic drivers of cancer. Cancer Res. 2017;77:3502–12.
77. Papin C, Denouel-Galy A, Laugier D, Calothy G, Eychene A. Modulation of kinase activity and oncogenic properties by alternative splicing reveals a novel regulatory mechanism for B-Raf. J Biol Chem. 1998;273:24939–47.
78. Leevers SJ, Paterson HF, Marshall CJ. Requirement for Ras in Raf activation is overcome by targeting Raf to the plasma membrane. Nature. 1994;369:411–4.
79. Fehrenbacher N, Bar-Sagi D, Philips M. Ras/MAPK signaling from endomembranes. Mol Oncol. 2009;3:297–307.
80. Selt F, Deiss A, Korshunov A, Capper D, Witt H, van Tilburg CM, et al. Pediatric targeted therapy: clinical feasibility of personalized diagnostics in children with relapsed and progressive tumors. Brain Pathol. 2016;26:506–16.

Affiliations

Florian Weinberg[1,2] · Ricarda Griffin[1] · Martina Fröhlich[3] · Christoph Heining[4,5,6] · Sandra Braun[1,2] · Corinna Spohr[1,7,8] · Mary Iconomou[1] · Viola Hollek[1] · Michael Röring[1] · Peter Horak[9,10] · Simon Kreutzfeldt[9,10] · Gregor Warsow[11,12] · Barbara Hutter[3] · Sebastian Uhrig[3,13] · Olaf Neumann[10,14] · David Reuss[10,15,16] · Dieter Henrik Heiland[17,18] · Christof von Kalle[19] · Wilko Weichert[20,21] · Albrecht Stenzinger[10,14] · Benedikt Brors[3,10] · Hanno Glimm[4,5,6] · Stefan Fröhling[9,10] · Tilman Brummer[1,2,22,23]

1 Institute of Molecular Medicine and Cell Research, Faculty of Medicine, University of Freiburg, Freiburg, Germany

2 Centre for Biological Signalling Studies BIOSS, University of Freiburg, Freiburg, Germany

3 Division of Applied Bioinformatics, German Cancer Research Center (DKFZ) and National Center for Tumor Diseases (NCT) Heidelberg, Heidelberg, Germany

4 Department of Translational Medical Oncology, NCT Dresden, Dresden, and DKFZ, Heidelberg, Germany

5 University Hospital Carl Gustav Carus, Technical University Dresden, Dresden, Germany

6 German Cancer Consortium (DKTK), Dresden, Germany

7 Faculty of Biology, University of Freiburg, Freiburg, Germany

8 Spemann Graduate School of Biology and Medicine (SGBM), University of Freiburg, Freiburg, Germany

9 Department of Translational Medical Oncology, NCT Heidelberg and DKFZ, Heidelberg, Germany

10 DKTK, Heidelberg, Germany

11 Omics IT and Data Management Core Facility, DKFZ, Heidelberg, Germany

12 Division of Theoretical Bioinformatics, DKFZ, Heidelberg, Germany

13 Faculty of Biosciences, Heidelberg University, Heidelberg, Germany

14 Institute of Pathology, Heidelberg University Hospital, Heidelberg, Germany

15 Department of Neuropathology, Institute of Pathology, Heidelberg University Hospital, Heidelberg, Germany

16 Clinical Cooperation Unit Neuropathology, German Cancer Research Center (DKFZ), German Consortium for Translational Cancer Research (DKTK), Heidelberg, Germany

17 Department of Neurosurgery, Medical Center, Faculty of Medicine, University of Freiburg, Freiburg, Germany

18 Translational NeuroOncology Research Group, Medical Center, Faculty of Medicine, University of Freiburg, Freiburg, Germany

19 Department of Translational Oncology, NCT Heidelberg and DKFZ, Heidelberg, Germany

20 Institute of Pathology, Technical University Munich, Munich, Germany

21 DKTK, Munich, Germany

22 Comprehensive Cancer Centre Freiburg, University of Freiburg, Freiburg, Germany

23 DKTK Partner Site Freiburg and DKFZ, Heidelberg, Germany